

Nitrogen-doped cobalt nanocatalysts for carbonylation of propylene oxide

Bo Zeng*, Lin Chen, Gangli Zhu, Bingxiao Yang, Chungu Xia*, Lin He*

State Key Laboratory for Oxo Synthesis and Selective Oxidation, Suzhou Research Institute of LICP, Lanzhou Institute of Chemical Physics (LICP), Chinese Academy of Sciences, Lanzhou, 730000, PR China

ARTICLE INFO

Keywords:

Carbonylation
Cobalt
Nanocatalysts
Supported
Propylene oxide

ABSTRACT

Nitrogen-doped cobalt nanoparticles loaded on porous supports were developed for ring-opening carbonylation of propylene oxide. The catalysts were prepared by simply pyrolysis of $\text{Co}(\text{OAc})_2/\text{phenanthroline}$ and supports. As proved by XPS combined with XRD and TEM characterizations, a higher amount of available Co-N sites were responsible for promoting the carbonylative activity. The selectivity of carbonylated products reached 93 %, which is comparable to previously reported cobalt carbonyl catalysts. The novel type of carbonylative catalyst also could be reused and revealed fine stability due to the continuous generation of active $[\text{Co}(\text{CO})_4]^-$ species during reaction.

1. Introduction

Carbonylation reactions, which introduce carbonyl compounds into organic and inorganic substrates, are used extensively in industry as illustrated by the bulk production of carbonylation products, such as acetic acid and butyl aldehyde [1]. Over the past few decades, dicobalt octacarbonyl ($\text{Co}_2(\text{CO})_8$) has been broadly reported as a highly active and selective homogeneous catalyst in several kinds of carbonylation reactions, such as hydroformylation [2], alkoxycarbonylation [3,4] and amidocarbonylation [5]. However, due to the dissociation of CO and oxidation of zero-valent cobalt, $\text{Co}_2(\text{CO})_8$ often requires carefully protection during preparation, storage, transportation and utilization [6,7]. It is necessary to develop a more stable and durable catalyst system for replacing the $\text{Co}_2(\text{CO})_8$ in carbonylation reactions.

β -Hydroxy esters are widely used in drugs [8] and serve as key intermediates in industrial production of value-added chemicals such as 1, 3-alkanediols [9], α , β -unsaturated esters [10] and poly(β -hydroxyalkanoates) [11]. Among the methodologies to synthesis β -hydroxy esters, the cobalt catalyzed alkoxycarbonylation of epoxides is comparatively efficient. To avoid direct use of the bothersome $\text{Co}_2(\text{CO})_8$, novel type of catalysts were developed, including developing ionic liquid [9,12], polymer and covalent triazine frameworks based cobalt tetracarbonyl ($[\text{Co}(\text{CO})_4]^-$) catalysts [13–15]. Due to the alkoxycarbonylation reaction starts with $[\text{Co}(\text{CO})_4]^-$ anion [16,17], these catalyst systems performed good reactivity as well as realized catalyst recycling to some extent. However, the essential problem that the direct use of labile carbonyl cobalt catalysts remained unsolved. For example, the preparation and utilization of imidazolium-CTF based $[\text{Co}(\text{CO})_4]^-$

catalysts were carefully conducted under protective atmosphere. More strictly, the reactant and solvent were prior dehydrated and deoxygenated so as to sustain the catalyst reactivity [12,14,15]. In order to meet the requirements of industrial production more possibly, the catalyst needs to be more practical and stable to adapt to more convenient operating conditions. Considering the possible decomposition of carbonyl cobalt catalysts, Hamasaki et al. reported a novel $\text{Au}/\text{Co}_3\text{O}_4$ catalyst, which realized the alkoxycarbonylation of epoxides via in-situ generation of fresh and active $\text{Co}_2(\text{CO})_8$ -like species during reaction process [6]. The recovery of the costly Au (0.6 mol% Au used) and catalyst recycle are technically demanding. In addition, the air-stable cobalt(II) halogen salts were employed as the precursor of $[\text{Co}(\text{CO})_4]^-$ for alkoxycarbonylation of epoxides [17]. However, the involved halogen and reductive metal, which accelerated the generation of active species [16], caused the catalyst system too complicated to understand their effects on reaction performances. Besides, the halogen is considered corrosive to reactors [18].

A variety of nitrogen-containing ligands (e.g. pyridine and imidazole) have broadly been utilized as promoters for activating the epoxides in homogeneous carbonylation of epoxides [17]. Correspondingly, the solid nitrogen-containing materials with the immobilized N species were also regarded as “solid ligands” [19]. It has been convinced that there are metal-nitrogen interactions when the metal nanoparticles were loaded on N-doped carbon materials (NCs) [20]. The NCs supported cobalt catalysts have been employed in diverse industrial transformations, including oxidations [21,22], reduction [23–25], H_2 generation [26], oxidative carbonylation [27] and FTS reactions [28]. In spite of extensive utilizations, to our knowledge, this

* Corresponding authors.

E-mail addresses: zengbo@licp.cas.cn (B. Zeng), cgxia@licp.cas.cn (C. Xia), helin@licp.cas.cn (L. He).

kind of catalysts have not yet been employed in the carbonylation of epoxides. Herein, we intend to develop and show the feasibility the solid nitrogen-doped cobalt nanocatalysts for the ring-opening carbonylation of propylene oxide (PO, which is used as a model epoxide because of its safety and easy accessibility) as highly active, selective, and recyclable catalysts.

2. Experimental

2.1. Catalyst preparation

The supported catalysts were prepared according to a procedure [29] reported previously with some modifications. Typically, the Co(OAc)₂·4H₂O (1.27 g, 5 mmol) and a stoichiometric ratio of 1,10-phenanthroline (Phen) were stirred in ethanol (200 mL) for approximately 15 min at room temperature. Then the whole reaction mixture was stirred at 60 °C for 1 h. The support was added and the mixture was stirred at room temperature overnight. The ethanol was removed by vacuum rotary evaporation and further dried in vacuo. The resultant solid sample was grinded to a fine powder which was transferred into a ceramic crucible and placed in the oven. After flushed with argon for ten minutes, the oven was heated to 800 °C at a rate of 10 °C min, and held at 800 °C for 2 h under argon atmosphere. The argon was constantly passed through the oven until it was cooled to room temperature. The as-prepared catalysts were denoted as Co-N_xC/support, where x represented Phen/cobalt ratios and support is the employed porous material. All catalysts were prepared according to cobalt loadings of 3.1 wt% in the as-synthesized catalysts by weight.

2.2. Characterizations

Transmission electron microscopy (TEM) and x-ray energy dispersive spectroscopy (EDX) measurements of the catalysts were recorded using a FEI JEM-1200-EX electron microscope equipped with a Super-X EDS and operated at an acceleration voltage of 200 kV. The BET surface area of catalysts (100 mg) were determined by nitrogen adsorption-desorption measurements using a Micromeritics Tristar 3000 sorptometer. X-ray diffraction (XRD) patterns of the ground samples were received on a DX-2700 diffractometer using CuK_α radiation ($\lambda = 0.154184$ nm). Diffraction data were collected between 5° and 90° (2 θ) with a resolution of 0.02°. The cobalt loadings of the catalysts before and after each reaction were determined by Inductively Coupled Plasma Optical Emission Spectrometer (ICP-OES) in a Thermo iCAP 6300 spectrometer after complete dissolution of the samples (ca. 100 mg) in a HNO₃/HF/HClO₄/HCl warm solution (4/4/3/5 vol ratio). X-ray photoelectron spectroscopy (XPS) of the catalysts was recorded on an AXIS ULTRA DLD spectrometer (Kratos) with a monochromatized Al K_α source (1486.7 eV). The measurement was performed at room temperature and a high vacuum of 10⁻⁸ Torr in analysis chamber. Elemental analysis for carbon, nitrogen and hydrogen was performed on a vario-EL III CHN elemental analyzer. Temperature programmed NH₃ desorption (NH₃-TPD) was performed in a quartz micro-reactor. The sample was swept by argon at 150 °C for 2 h to remove the physically adsorbed NH₃. The TPD experiments were then carried out in an argon flow (40 mL·min⁻¹) by heating from 150 °C to 700 °C with a rate of 10 °C min⁻¹. Desorption signals of NH₃ were recorded by Shanghai GC-920 equipped with a thermal conductivity detector (TCD). The filtrate of after reaction were immediately detected by Fourier transformed infrared spectra (FT-IR), which were measured on a Thermo Scientific Nicolet 870 Microscope. The scanning scope is 400–4000 cm⁻¹ and the spectra were acquired in transmission mode.

2.3. Catalytic reactions

All reaction preparing process was conducted in the presence of air and the reagents were used directly without further treatment. The

carbonylation experiments were carried out in a 15 ml stainless steel autoclave equipped with magnetic stirring. In a typical experiment, methanol (0.4 mL), THF (1.6 mL), pyrazole (0.03 mmol), catalyst, dodecane (internal standard) and propylene oxide (0.55 mmol) were successively charged into the reactor. Then the autoclave was precooled before purged three times with carbon monoxide (CO 99.999 %) to possibly reduce the PO lost by the vented gasses [30], which ensured the carbon balance of each analysis in the range of 95%–100%. After the reaction, the autoclave was cooled and CO was slowly vented. The samples were taken out of the reaction solution and passed through a polypropylene membrane filter. All the components were quantitatively and qualitatively analyzed by gas chromatograph (Agilent 7890 with a HP-5 capillary column and FID detector) and GC-MS (Shimadzu, QP-2010 SE).

3. Results and discussion

3.1. Catalytic performances

The catalytic ring-opening carbonylation of PO with CO and methanol produces the methyl-3-hydroxybutyrate (MHB), 3-mydroxybutyric acid (HBA) and methyl 3-hydroxy-2-methyl-propanoate (MMP). Other by-products are ethers, including 2-methoxy propanol, 2-hydroxymethylpropylether, 2,2-dimethoxypropane and 1,2-dimethoxypropane, which are all produced by the nucleophilic reaction of one or two molecular of methanol with PO rather than the insertion of CO [31]. This result can be reasonably explained by the generation of solvated H⁺ in mixture of cobalt carbonyls and methanol under high pressure of CO [16,32]. In order to highlight the carbonylated products, the selectivity of ethers was listed as integral without splitting to each value in the following tables and figures.

Porous materials are considered as superior supports for catalysts, because their extensive pores could confine metal particles to the nanometer size and are beneficial for mass transfers in reactions [33,34]. In the absence of porous materials, the catalyst Co-N₁C (entry 2 in Table 1) exhibited slight reactivity as well as a low carbonylative selectivity. The additional supports remarkably improved activity, which may be attributed to the enhanced cobalt dispersion as observed in TEM images (Fig. S1a and c). As compared with series of supports (entry 3–11), the SiO₂ best contributed to the carbonylative selectivity, which illustrated that the surface properties of support greatly affected the reaction performances (detailed discussion please see supporting information). Although the TiO₂, α -Al₂O₃ and γ -Al₂O₃ supported catalysts showed comparatively high activity, the selectivity of carbonylated products were fairly low. This behavior might derive from a higher extent of etherification between PO and methanol on these acidic supports (Fig. S3) [35]. It is suggested that the support should be less acidic to suppress the formation of ethers, which cuts down selectivity of carbonylated products.

Subsequently, the reaction temperature (50–100 °C, Fig. S4), CO pressure (3–8 MPa, Fig. S5) and reaction time (5–60 h, Fig. S6) were screened for the catalyst Co-N₁C/SiO₂. The results proved that the optimal reaction temperature, CO pressure and reaction time should be 70 °C, 6 MPa and 40 h, respectively. Several kinds of solvents such as alcohols, hydrocarbons, esters and ethers were tested (Table S2). From a survey of literatures, methanol had been the most commonly employed as both the solvent and reactant in this reaction [14,31,36]. While in our reaction system, the ethers, especially THF, revealed obviously higher selectivity to carbonylated products than others. This behavior might ascribe to the donating ability of ethers [37].

The addition of extra N-donating ligands were also investigated to further promote the carbonylative activities [31,36,38]. Without any promoter, the catalyst Co-N₁C/SiO₂ exhibited 88 % of PO conversion with total selectivity towards carbonylated products (MHB, MHA plus MMP) of 80 % (entry 12). The Phen and 2,2'-dipyridyl led to lower PO conversion and carbonylative selectivity instead (entry 13 and 14). The

Table 1
The promoter and support effects on ring-opening carbonylation of PO^a.

Entry	Support	Promoter	PO Conv. (mol%) ^b	Selectivity (mol%) ^b	
				Carbonylated products (MHB/HBA/MMP)	Ethers
1	SiO ₂	Pyrazole	93	93 (84/7/2)	
2	–	Pyrazole	15	34 (33/1/0)	
3	BN	Pyrazole	59	42 (39/2/1)	
4	C ₃ N ₄	Pyrazole	87	64 (58/4/2)	
5	Graphite	Pyrazole	68	48 (43/3/2)	
6	B ₄ C	Pyrazole	42	64 (57/5/2)	
7	CeO ₂	Pyrazole	23	47 (41/4/2)	
8	TiO ₂	Pyrazole	86	35 (29/4/2)	
9	a-Al ₂ O ₃	Pyrazole	90	22 (21/1/0)	
10	r-Al ₂ O ₃	Pyrazole	> 99	5 (5/0/0)	
11	Hydrotalcite	Pyrazole	66	51 (46/3/2)	
12	SiO ₂	–	88	80 (72/6/2)	
13	SiO ₂	Phen	36	19 (17/2/0)	
14	SiO ₂	2,2'-Dipyridyl	40	59 (55/3/1)	
15	SiO ₂	3-Hydroxypyridine	98	82 (73/7/2)	
16	SiO ₂	Imidazole	90	79 (70/7/2)	

^a 0.05 g of catalyst (S/Co = 20).

^b Determined by gas chromatograph with dodecane as an internal standard.

large steric hindrance from double six-member rings might give rise to this unfavourable effect. However, the single-ring promoters with lower steric hindrance facilitated the carbonylation, in which the 3-hydroxypyridine contributed most to catalytic activity and pyrazole favored both 93 % of the PO conversion and carbonylative selectivity. This value is comparable with previously reported Co₂(CO)₈ catalyst [36,39].

3.2. Effect of Phen/Co ratios

A correlation between the Phen/Co ratios and catalytic performance was established as plotted in Fig. 1. The content of immobilized N species in catalysts which were previously regarded as “solid ligands” to metals [19] could readily be modulated by altering Phen/Co ratios. The curves verified that the Phen/Co ratios notably impacted reaction behaviors, with the optimal Phen/Co ratio of 1. This trend might be attributed to the changed cobalt situation when the surface cobalt atoms were coordinated with N species. The extra addition of pyrazole best

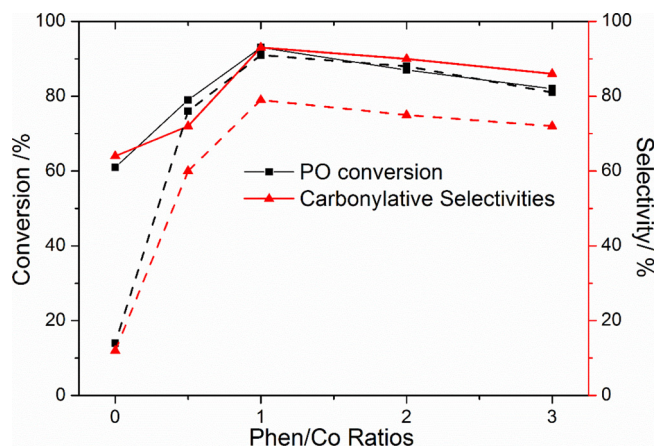


Fig. 1. Effects of Phen/Co ratios on carbonylation of PO. Reaction conditions: T = 70 °C, P(CO) = 6 MPa, t = 40 h, S/Co = 20. Solid lines: Pyrazole addition; Dash lines: Without pyrazole addition.

enhanced the carbonylative activity of the catalyst Co-N₁C/SiO₂, which especially illustrated the promoting effects of N species to cobalt.

The XPS spectra of catalyst with different Phen/Co ratios were conducted to point out the interaction between Co and N species. In the cobalt region (Fig. 2a), the typical binding energy of Co2p_{3/2} and Co2p_{1/2} at 781 eV and 796 eV with the satellite peaks at 786.7 eV and 802.8 eV are characteristics for Co²⁺ species [40]. The lower binding energies were observed when the Phen/Co ratios were higher than 1, probably because more N atoms are coordinated with Co. Higher binding energies might result from combination of Co with O atoms, which especially reflected in the sample Co-N₀C/SiO₂. As depicted in Fig. 2b, three distinct peaks were observed in the N1s spectra with an electron binding energy of 399.0 eV, 400.8 eV and 402.3 eV except the Co-N₀C/SiO₂, which had no N component. These peaks could be respectively assigned to pyridine-type nitrogen (N bound to the Co ions), to pyrrolic nitrogen (nitrogen contributing two electrons to the carbon) and to ammonium species like NH₄⁺ or R-NH₃⁺ [41]. The relative amount of the N species was further determined from the peak areas after division by the element-specific Scofield factor and the transmission function of the spectrometer (Table 2). It is concluded that the percentages of Co-bounded N raised and followed by a slight decline with the increased Phen/Co ratios. The highest percentage of Co-bounded N appeared on Co-N₁C/SiO₂, which revealed to the optimum catalytic activity and carbonylative selectivity (Fig. 1).

One could draw from Table 2 that the Co-N₃C/SiO₂ presented the most content of pyridinic nitrogen, while did not exhibit the highest carbonylative activity. This abnormal behavior prompted us to find out whether the cobalt dispersion affected the activity as well. Thus the XRD patterns and TEM images were combined to further discern the cobalt particle sizes of the catalysts. It is well known that the changes of XRD peak intensity corresponded to the variation of cobalt particle sizes (Fig. 3) [42]. The slightest peaks of Co-N₁/CSiO₂ proved the highest cobalt dispersion (the smallest particle size), which was consistent with TEM images (Fig. S1b, c and d). As a result, it is reasonable to infer that the optimal catalyst activity of Co-N₁C/SiO₂ primarily derived from its highest cobalt dispersion, which provided the maximum amount of available surface Co-N sites.

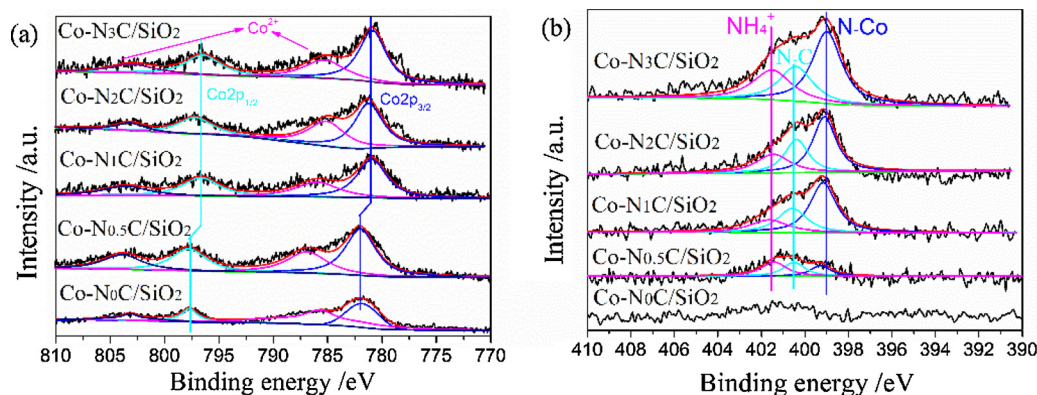


Fig. 2. XPS spectra of the Co2p (a) and N1s (b) region level for the catalysts with different Phen/Co ratios.

Table 2
N forms and contents on catalysts.

Catalyst	N wt % ^a	Percentage of N forms % ^b		
		N-pyridinic	N-pyrrolic	N-ammonium
Co-N ₀ C/SiO ₂	0	–	–	–
Co-N _{0.5} C/SiO ₂	0.16	25	34	41
Co-N ₁ C/SiO ₂	0.73	52	28	19
Co-N ₂ C/SiO ₂	0.82	51	30	19
Co-N ₃ C/SiO ₂	1.09	48	26	26

^a Measured by elemental analysis.

^b Calculated from XPS spectra.

Table 3
Catalytic run of Co-N₁C/SiO₂ in the carbonylation of PO^a.

Run	PO conv. (mol%) ^b	Selectivity (mol%) ^b	
		Carbonylated products (MHB/HBA/MMP)	Ethers
1	93	93(84/7/2)	7
2	91	92(82/8/2)	8
3	88	91(81/8/2)	9
4	86	89(78/9/2)	11
5	77	85(73/11/1)	15

^a Reaction conditions: T = 70 °C, P(CO) = 6 MPa, t = 40 h, S/Co = 20.

^b Determined by gas chromatograph with dodecane as an internal standard.

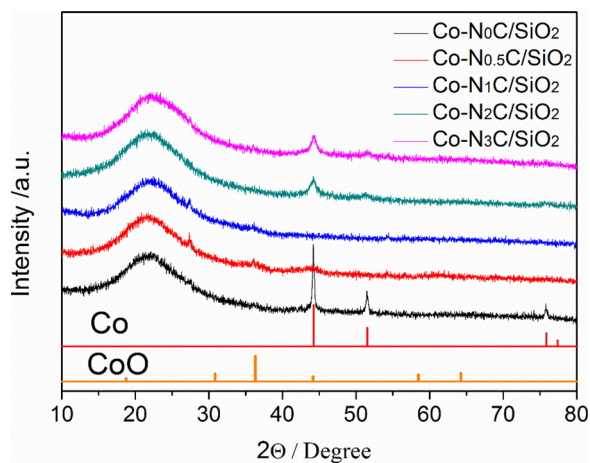


Fig. 3. XRD patterns of samples with different Phen/Co ratios.

3.3. Catalyst reusability

To understand the stability of Co-N₁C/SiO₂ during reaction, the catalyst after each run was simply separated by filtration, washed with methanol and dried under air at 60 °C. To our delight, the catalytic system could be reused at least 4 times, with a minor loss of selectivity and conversion (Table 3). The good reusability of this kind of catalyst could probably be attributed to the in-situ continuous generation of the active [Co(CO)₄][−] as verified by FT-IR analysis with a typical peak corresponding to C = O absorption at approximately 1888 cm^{−1} (Fig. S7) [43]. It is deduced that the [Co(CO)₄][−] in the filtrate derived from a certain extent of cobalt leaching which happens on the surface of nanoparticles. The gradually decreases of cobalt loadings after each run from the ICP-OES (Table S3) further proved our inference. The leaching process would give rise to smaller cobalt particle size after five runs than the freshly prepared catalyst, which was also demonstrated by

TEM images (Fig. S1c and e). The EDX analysis and ICP-OES jointly confirmed the existence of remaining cobalt after five runs (Fig. S1g and Table S3). It is calculated that there was a remaining cobalt of 57.8 % after five runs as compared with reaction before, which made us to believe that the catalyst could further be reused.

3.4. Carbonylative mechanism

Based on our results and the previous understanding [9,14,31], we propose a plausible mechanism for carbonylation of PO in our catalyst system as depicted in Fig. 4. Under the high pressured CO atmosphere, the surface cobalt atoms of catalyst firstly coordinated with CO to generate [Co(CO)₄][−] species, which were subsequently reacted with the acidic proton from pyrazole in solvents or surface N–H species from catalyst to produce the active HCo(CO)₄ [16]. The H⁺ activated PO followed by nucleophilic attack of [Co(CO)₄][−] to form the cobalt – alkyl bonded intermediates (a and b). Intermediate a converted to c via the intramolecular migratory insertion of CO the Co-Calkyl bond. The MHB formation happened through the uptake of CO from intermediate c followed by addition of methanol to d. The MMP generated from b via a similar route. It is proposed that the HBA derives from the carbonylation of PO with CO followed by reacting with water [44], which comes from the undehydrated solvent and reactants.

3.5. Activity comparison

It's expected that the catalytic activity of supported cobalt nanocatalysts were comparatively inferior to previously reported cobalt carbonyl catalysts [3,4,9–15,31,38]. In fact, the active [Co(CO)₄][−] inherently existed or fast generated under reaction conditions for those cobalt carbonyl catalysts [16]. According to each reuse of our catalysts, the generation of active [Co(CO)₄][−] proceeded slowly by leaching of the surface cobalt nanoparticles, thus exhibited comparatively low activity. As compared with Au/Co₃O₄ catalyst, which also realized the carbonylative activity by cobalt leaching [6], the Co-N₁C/SiO₂ revealed

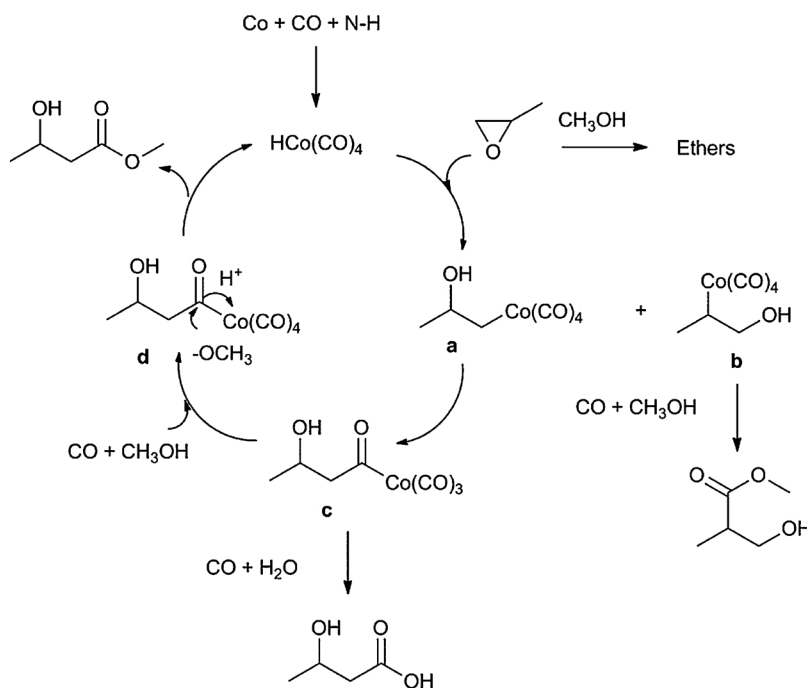


Fig. 4. Proposed mechanism for PO carbonylation reactions.

better activity.

4. Conclusions

In summary, we achieved to develop a series of supported cobalt nanocatalysts for efficient ring-opening carbonylation of epoxides. The highest amount of available Co-N sites were proved to contribute to carbonylative reactions, with the optimal conversion and total selectivity of carbonylated products (MHB, MHA and MMP) of 93 %. Moreover, the reaction stability was realized via a continuous in-situ generation of active $[\text{Co}(\text{CO})_4]^-$ species. This type of catalyst might be a good candidate for industrial-scale carbonylation of epoxides due to its fine reactivity, facile reusability and superior air stability. Further measures to improve the reaction rate and selectivity towards a single carbonylated product are still underway.

CRedit authorship contribution statement

Bo Zeng: Conceptualization, Writing - original draft. **Lin Chen:** Methodology. **Gangli Zhu:** Data curation, Formal analysis. **Bingxiao Yang:** Investigation. **Chungu Xia:** Supervision, Writing - review & editing. **Lin He:** Conceptualization, Funding acquisition, Writing - review & editing.

Declaration of Competing Interest

The authors declare that they have no known competing financial interests or personal relationships that could have appeared to influence the work reported in this paper.

Acknowledgements

The authors gratefully appreciate the financial support from the National Natural Science Foundation of China (grant no. 21802152, 21673260, 21373248 and 21802151) and the Foundation research project of Jiangsu Province (grant no. BK20171242 and BK20180249). Thanks also go to the anonymous reviewers for their advice and suggestions.

Appendix A. Supplementary data

Supplementary material related to this article can be found, in the online version, at doi:<https://doi.org/10.1016/j.mcat.2020.111109>.

References

- [1] K. Nakano, K. Nozaki, *Top. Organomet. Chem.* 18 (2006) 223–238.
- [2] H. Adkins, G. Kresk, *J. Am. Chem. Soc.* 71 (1949) 3051–3055.
- [3] J. Eisenmann, R. Yamartino, J.J. Howard, *J. Org. Chem.* 26 (1961) 2102–2104.
- [4] K. Hintterding, E.N. Jacobsen, *J. Org. Chem.* 64 (1999) 2164–2165.
- [5] R.M. Gómez, A. Cabrera, C.G. Velázquez, *J. Mol. Catal. A.* 274 (2007) 65–67.
- [6] A. Hamasaki, A. Muto, S. Haraguchi, X. Liu, T. Sakakibara, T. Yokoyama, M. Tokunaga, *Tetrahedron Lett.* 52 (2011) 6869–6872.
- [7] F. Hebrard, P. Kalck, *Chem. Rev.* 109 (2009) 4272–4282.
- [8] K. Tieu, C. Perier, C. Caspersen, P. Teismann, D.C. Wu, S.D. Yan, A. Naini, M. Vila, V. Jackson-Lewis, R. Ramasamy, *J. Clin. Invest.* 112 (2003) 892–901.
- [9] Z. Guo, H. Wang, Z. Lv, Z. Wang, T. Nie, W. Zhang, *J. Organomet. Chem.* 696 (2011) 3668–3672.
- [10] J. L. Dever, P. Ambler. U.S. Patent 3182077 (1962).
- [11] K. Sudesh, H. Abe, Y. Doi, *Prog. Polym. Sci.* 25 (2000) 1503–1555.
- [12] F. Deng, B. Hu, W. Sun, J. Chen, C. Xia, *Dalton Trans.* 38 (2007) 4262–4267.
- [13] Y. Liu, Y. Wang, H. Lu, S. Liang, B. Xu, Y. Fan, *Chem. Asian J.* 11 (2016) 3159–3164.
- [14] S. Rajendiran, K. Park, K. Lee, S. Yoon, *Inorg. Chem.* 56 (2017) 7270–7277.
- [15] S. Rajendiran, G.H. Gunasekar, S. Yoon, *New J. Chem.* 42 (2018) 12256–12262.
- [16] M.F. Mirbach, M.J. Mirbach, *J. Mol. Catal.* 32 (1985) 59–75.
- [17] J. Xu, X. Wu, *J. Org. Chem.* 84 (2019) 9907–9912.
- [18] C.C. Busby, R.P. Tucker, J.E. McCauley, *J. Nucl. Mater.* 55 (1975) 64–82.
- [19] L. He, F. Weniger, H. Neumann, M. Beller, *Angew. Chem. Int. Ed.* 55 (2016) 12582–12594.
- [20] R. Arrigo, M. Schuster, Z. Xie, Y. Yi, G. Wowsnick, L. Sun, K. Hermann, M. Friedrich, P. Kast, M. Hävecker, A. Knop-Gericke, R. Schlög, *ACS Catal.* 5 (2015) 2740–2753.
- [21] J. Deng, H. Song, M. Cui, Y. Du, Y. Fu, *ChemSusChem* 7 (2014) 3334–3340.
- [22] R.V. Jagadeesh, H. Junge, M.M. Pohl, J. Radnik, A. Brückner, M. Beller, *J. Am. Chem. Soc.* 135 (2013) 10776–10782.
- [23] T. Cheng, H. Yu, F. Peng, H. Wang, B. Zhang, D. Su, *Catal. Sci. Technol.* 6 (2016) 1007–1015.
- [24] F. Chen, A.E. Surkus, L. He, M.M. Pohl, J. Radnik, C. Topf, K. Junge, M. Beller, *J. Am. Chem. Soc.* 137 (2015) 11718–11724.
- [25] S. Pisiewicz, T. Stemmler, A.E. Surkus, K. Junge, M. Beller, *ChemCatChem* 7 (2015) 62–64.
- [26] J. Yu, W. Zhou, T. Xiong, A. Wang, S. Chen, B. Chu, *Nano Res.* 10 (2017) 2599–2609.
- [27] J. Li, D. Tu, Y. Li, W. Wang, Q. Yu, J. Yang, J. Lu, *Appl. Catal. A. Gen.* 549 (2018) 112–116.
- [28] S. Li, N. Yao, F. Zhao, X. Li, *Catal. Sci. Technol.* 6 (2016) 2188–2194.
- [29] D. Banerjee, R.V. Jagadeesh, K. Junge, M.M. Pohl, J. Radnik, A. Brückner, M. Beller,

- Angew. Chem. Int. Ed. 53 (2014) 4359–4363.
- [30] Y.D.Y.L. Getzler, V. Mahadevan, E.B. Lobkovsky, G.W. Coates, *J. Am. Chem. Soc.* 124 (2002) 71174–71175.
- [31] J. Liu, J. Chen, C. Xia, *J. Mol. Catal. A: Chem.* 250 (2006) 232–236.
- [32] R. Tuba, L. Mika, A. Bodor, Z. Pusztai, I. Tóth, I.T. Horváth, *Organometallics* 22 (2003) 1582–1584.
- [33] S. Pariente, N. Tanchoux, F. Fajula, *Green Chem.* 11 (2009) 1256–1261.
- [34] A. Primo, F. Quignard, *Chem. Commun.* 46 (2010) 5593–5595.
- [35] S. Pariente, N. Tanchoux, F. Fajula, *Green Chem.* 11 (2009) 1256–1261.
- [36] E. Drent, E. Kragtwijk, *European Patent EP 577206* (1994).
- [37] T.L. Church, Y.D.Y.L. Getzler, G.W. Coates, *J. Am. Chem. Soc.* 128 (2006) 10125–10133.
- [38] S.E. Denmark, M. Ahmad, *J. Org. Chem.* 72 (2007) 9630–9634.
- [39] J. Liu, H. Wu, L. Xu, J. Chen, C. Xia, *J. Mol. Catal. A: Chem.* 269 (2007) 97–103.
- [40] V. Papaefthimiou, T. Dintzer, V. Dupuis, A. Tamion, F. Tournus, A. Hillion, D. Teschner, M. Hävecker, A. Knop-Gericke, R. Schlögl, S. Zafeiratos, *ACS Nano* 5 (2011) 2182–2190.
- [41] R.V. Jagadeesh, H. Junge, M.M. Pohl, J. Radnik, A. Brückner, M. Beller, *J. Am. Chem. Soc.* 135 (2013) 10776–10782.
- [42] B. Zeng, B. Hou, L. Jia, J. Wang, C. Chen, Y. Sun, D. Li, *ChemCatChem* 5 (2013) 3794–3801.
- [43] M. Allmendinger, M. Zintl, R. Eberhardt, G.A. Luinstra, F. Molnar, B. Rieger, *J. Organomet. Chem.* 689 (2004) 971–979.
- [44] S. Rajendiran, G. Park, S. Yoon, *Catalysts* 7 (2017) 228–233.